

Electrostatic interactions in concentrated protein solutions

Shradha Mishra* and Jeremy D. Schmit†

Department of Physics, Kansas State University, Manhattan, KS 66506, USA

Abstract

We present an approximate method for calculating the electrostatic free energy of concentrated protein solutions. Our method uses a cell model and accounts for both the coulomb energy and the entropic cost of Donnan salt partitioning. The former term is calculated by linearizing the Poisson-Boltzmann equation around a nonzero average potential, while the second term is calculated using a jellium approximation that is empirically modified to reproduce the dilute solution limit. When combined with a short-ranged binding interaction, calculated using the mean spherical approximation, our model reproduces osmotic pressure measurements of bovine serum albumin solutions. We also use our free energy to calculate the salt-dependent shift in the critical temperature of lysozyme solutions and show why the predicted salt partitioning between the dilute and dense phases has proven experimentally elusive.

PACS numbers:

* shradha@phys.ksu.edu, Present address: Department of physics, Indian Institute of technology Kharagpur, Kharagpur India, 721302

† schmit@phys.ksu.edu

I. INTRODUCTION.

Dense protein solutions are encountered in the cytoplasm and *in vitro* situations like pharmaceutical formulations, crystallization screens, and ultrafiltration [1–3]. In all these cases, the stability of the solution depends on sufficient electrostatic repulsion to overcome the short-range attraction of H-bond, hydrophobic, and van der Waals interactions. Electrostatic interactions are easily adjusted through changes in the pH or salt concentration providing a convenient experimental means to manipulate the phase behavior. However, they are difficult to model theoretically due to the long range nature of the coulomb force and the nonlinearity of salt screening. Because of this, most theoretical work on protein-protein interactions has focused on dilute solution properties where the electrostatic free energy is dominated by the coulomb energy and can be treated using two-body potentials [4–6]. We have recently shown that the electrostatic free energy of protein association is dominated by the change in salt ion entropy, which renders the net interaction strongly non-pairwise [7]. In this paper we extend these results in order to model electrostatic effects in non-ideal protein solutions.

We test our theory against pH dependent measurements of the osmotic pressure and salt effects on the liquid-liquid phase separation of protein solutions. The osmotic pressure provides a direct test of the effective interparticle repulsion, while the latter phenomenon has attracted considerable attention due to the finding that fluctuations associated with the liquid-liquid critical point have been shown to accelerate crystal nucleation [8]. Liquid-liquid separation is analogous to the liquid-vapor coexistence in small molecules except that in proteins the liquid-liquid binodal is found entirely below the solid (crystal) solubility line due to the short range of the protein-protein attractive forces [9, 12]. Previous work has primarily focused on temperature as a means of controlling a phase behavior. However, temperature is a poor variable in protein systems because the accessible temperature range is limited to $\sim 20\%$ due to the freezing point of water and the thermal denaturation of the proteins. Our work shows how pH and salt can be used to manipulate the phase boundary into the accessible range.

II. MODEL

Our calculations are based on the following free energy of the ternary protein-salt-solvent system

$$f(\eta) = F(\eta)/N = f_{\text{hc}}(\eta) + f_{\text{att}}(\eta) + f_{\text{salt}}(\eta) + f_{\text{coulomb}}(\eta) \quad (1)$$

where $f(\eta)$ is the total free energy per protein as function of protein concentration η . f_{hc} is the mixing entropy of spherical proteins interacting by a hard core potential, f_{att} is the free energy due to short range attractions between the proteins, f_{salt} is the mixing entropy of the salt ions, and f_{coulomb} is the coulomb energy of the system. These terms are explicit functions of $\eta = N\sigma^3/6V$, the volume fraction occupied by the proteins, where σ is the protein diameter and N/V is protein number density. We discuss each of these terms in detail below.

A. Free energy of attractive spheres

The terms f_{hc} and f_{att} represent the free energy of a solution of attractive spheres. We adopt the attractive Yukawa potential to describe the short range interaction

$$U(r) = \begin{cases} \infty & r \leq \sigma; \\ -\epsilon(T) \frac{\exp[-z(r-\sigma)]\sigma}{r} & r > \sigma \end{cases} \quad (2)$$

where z is a parameter describing the range of interaction, σ is the hard sphere diameter, and ϵ is the temperature dependent strength of interaction. Following previous work [13, 14], we take $z = 4$ reflecting the short range nature of the hydrophobic and H-bond interactions that dominate protein-protein attractions.

Eq. 2 gives the binding energy of a two-body protein-protein interaction as a function of the center-to-center distance r . In order to derive macroscopic properties of the protein solution, we need to know the average binding energy per particle as a function of the protein concentration. We obtain this using the Mean Spherical Approximation [15, 16] the mean spherical approximation (MSA) is the method used to obtain the analytical solution of the radial distribution function of particles. The thermodynamic properties obtained from the MSA are in good agreement with results obtained from the Monte Carlo simulation.

Within this approximation the binding energy density is [14, 17]

$$f_{\text{att}} = \frac{\alpha_0}{\Phi_0} \beta \epsilon - \frac{z^3}{6\eta} \left[\mathcal{F}(X) - \mathcal{F}(Y) - (X - Y) \frac{d\mathcal{F}(Y)}{dY} \right] \quad (3)$$

where X and Y are the variable defined in A9 and A10. z is the parameter for range of interaction in the Yukawa potential and η is the volume fraction of the proteins. α_0 , Φ_0 , $\mathcal{F}(X)$ and its first derivative are defined in Eqs. A2, A5, A12 and A13. This binding energy is partially offset by the loss of translational entropy at the high concentration. This contribution is given by the Carnahan-Starling expression [18]

$$f_{\text{hc}}(\eta)/k_{\text{B}}T = \eta^2 \frac{4 - 3\eta}{(1 - \eta)^2}. \quad (4)$$

Advantage of using MSA for our case is that, we get an expression for free energy density in terms of density or volume fraction η of protein. We can compute equation of state, osmotic pressure and many other thermodynamic quantities using this free energy density. MSA is based on the inverse temperature expansion of the free energy, hence it gives better result for higher temperatures. In our phase coexistence curve 6 and 7 we find our theoretical curves are more promising for large salt or when we have larger critical. temperautre.

B. Electrostatic terms

To solve for the electrostatic free energy, we adopt a cell model [19] in which each protein is surrounded by a spherical shell of solvent of radius b . The thickness of this solvent layer is chosen to reproduce the volume fraction occupied by the protein $\eta = (\sigma/2b)^3$. We assume a protein solution in osmotic equilibrium with a reservoir of symmetric, monovalent salt of concentration c_s . The proteins carry a charge qe_p , where e_p is the proton charge, that we take to be uniformly distributed over their spherical surface. The protein charge will perturb the salt ion concentration resulting in a local enrichment of counterions and a local depletion of coions. The extent of this ionic perturbation is a competition between the coulomb interaction of the salt ions with the electrostatic potential Φ and the entropic cost of enriching/depleting the counterion/coion populations. These considerations are reflected in the electrostatic free energy $f_{\text{ES}} = f_{\text{coulomb}} + f_{\text{salt}}$ where

$$f_{\text{coulomb}} = \frac{\epsilon}{2} \int_V (\nabla \Psi)^2 d^3 \mathbf{r} \quad (5)$$

$$f_{\text{salt}}/k_{\text{B}}T = \int_{V'} [c_+ \ln(c_+/c_s) - c_+ + c_s] + [c_- \ln(c_-/c_s) - c_- + c_s] d^3 \mathbf{r}, \quad (6)$$

where c_{\pm} are the local cation/anion concentrations, V is the cell volume, V' is the solvent accessible cell volume, and ε is the local permeability which we take to be $80\varepsilon_0$. The electrostatic potential can be expressed in terms of the charge distribution using the Poisson equation

$$-\nabla \cdot (\varepsilon \nabla \Psi(\mathbf{r})) = \rho_p(\mathbf{r}) + e_p(c_+(\mathbf{r}) - c_-(\mathbf{r})) \quad (7)$$

where ρ_p is the charge density of the protein. The ion concentrations can be found by minimizing f_{ES} with respect to c_{\pm} after integrating Eq. 5 by parts and applying Eq. 7. This resulting concentrations are

$$c_{\pm}(\mathbf{r}) = c_s e^{\mp e_p \Psi(\mathbf{r})/k_B T}, \quad (8)$$

which, with Eq. 7, gives the well known Poisson-Boltzmann equation

$$-\nabla \cdot (\varepsilon \nabla \Psi(\mathbf{r})) = -\rho_p(\mathbf{r}) - e_p c_s (e^{-e_p \Psi(\mathbf{r})/k_B T} - e^{e_p \Psi(\mathbf{r})/k_B T}). \quad (9)$$

Our strategy is to develop approximate solutions of Eq. 9 that can be used in Eqs. 5 and 6 to calculate the free energy as a function of protein concentration, charge, and salt concentration.

Within the cell geometry, the Poisson-Boltzmann equation has the approximate solution

$$\begin{aligned} \Psi(x) &= \phi(x) + \phi_0 \\ &= C \left(\frac{e^{\beta-x}(\beta-1)}{x} + \frac{e^{x-\beta}(\beta+1)}{x} \right) - \tanh \phi_0 + \phi_0, \end{aligned} \quad (10)$$

where $\alpha = (\cosh \bar{\phi})^{1/2} \kappa \sigma / 2$, $\beta = (\cosh \bar{\phi})^{1/2} \kappa b$ and C is a constant defined in the appendix. Eq. 10 is derived by linearizing the Poisson-Boltzmann equation around a reference potential ϕ_0 ($\phi_0 = 0$ in the Debye-Huckel solution). The nonzero reference is necessary to model concentrated solutions of charged proteins, where the Donnan effect ensures that the potential never approaches zero.

Eq. 10 can be used with Eq. 5 to determine the coulomb energy per particle. A straightforward integration yields (see appendix)

$$\begin{aligned} f_{\text{coulomb}} &= -2C^2 \beta^3 + \frac{C^2}{\alpha} ((\beta-1)e^{-\alpha+\beta} + (\beta+1)e^{\alpha-\beta})^2 \\ &\quad - \frac{C^2}{2} ((\beta+1)^2 e^{2(\alpha-\beta)} - (\beta-1)^2 e^{-2(\alpha-\beta)} - 4(\beta^2-1)\alpha) \end{aligned} \quad (11)$$

To compute f_{salt} we first combine Eqs. 6 and 8 to obtain

$$f_{\text{salt}}/k_B T = 2c_s \int_{V'} \left[\left(\frac{e_p \phi}{k_B T} \right) \sinh \left(\frac{e_p \phi}{k_B T} \right) - \cosh \left(\frac{e_p \phi}{k_B T} \right) + 1 \right] d^3 \mathbf{x} \quad (12)$$

This expression does not lend itself to direct integration, however, at high protein concentrations the potential varies weakly in the voids between proteins and it is reasonable to replace it with an average value $\phi(\mathbf{x}) \rightarrow \bar{\phi}$ (the jellium approximation) so that c_{\pm} are constant [20]. Charge neutrality requires

$$q = -v_{\text{ion}}(c_+ - c_-) \quad (13)$$

$$= 2v_{\text{ion}}c_s \sinh(e\bar{\phi}/k_B T) \quad (14)$$

$$\frac{e\bar{\phi}}{k_B T} = \sinh^{-1} \frac{q}{2v_{\text{ion}}c_s}, \quad (15)$$

where v_{ion} , the solvent volume associated with each protein, is given by

$$v_{\text{ion}} = v_p \left(\frac{1}{\eta} - 1 \right), \quad (16)$$

where $v_p = \pi\sigma^3/6$ is the volume of a single protein.

Combining Eqs. 6 and 15 we find an expression for the salt entropy per protein at high protein concentrations

$$f_{\text{salt}}/Nk_B T = q(\sinh^{-1} \xi - \sqrt{1 + \xi^{-1}} + \xi^{-1}) \quad (17)$$

where $\xi = q/2v_{\text{ion}}c_s$. This expression is an excellent approximation for high concentration solutions, but fails in the dilute limit where it erroneously predicts that the entropic cost of the ion screening layers approaches zero. The problem can be traced to Eq. 16 which implies that the ion screening layer can become arbitrarily large. In reality, in dilute solutions the screening layer is confined to a shell with a thickness on the order of a Debye length. Because of this, the salt entropy will saturate at a minimum value when the concentration drops below a critical value η_0 . This behavior can be obtained from our model by a numerical integration of Eq. 6 with the potential given by 10. However, a more computationally efficient solution is to modify Eq. 16 to give the correct asymptotic behavior. This can be done with the following functional form

$$v_w^{\text{eff}} = v_p \left(\frac{1}{(\eta^n + \eta_0^n)^{1/n}} - 1 \right). \quad (18)$$

Here n and η_0 are adjustable parameters that give optimal results when $n = 5$ and $\eta_0 = (1 + 3.8/\kappa\sigma)^3$ where κ^{-1} is the Debye screening length. Fig. 1 shows an excellent agreement in the salt entropy calculated using these two methods. Therefore, the remainder of the paper will utilize the more efficient effective water shell calculation of salt entropy.

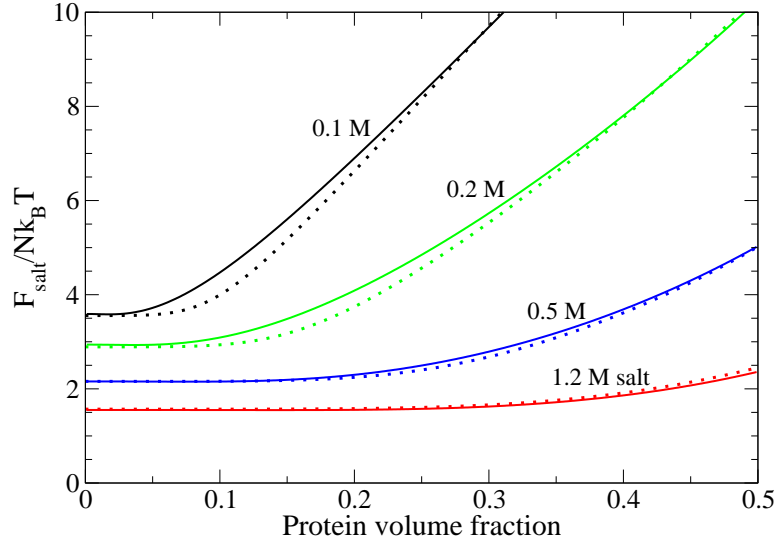


FIG. 1: Comparison of two methods for calculating the salt entropy per particle. Solid lines show a numerical integration of Eq. 6 with the potential given by Eq. 10. Dashed lines show Eq. 17 with the screening layer volume given by 18. $\sigma/2 = 16\text{nm}$, $b = (\sigma/2 + 1.9/\kappa)$, $q = 10.3$. The dashed lines have been shifted by an unimportant constant to facilitate comparison.

III. RESULTS AND DISCUSSION

A. Osmotic pressure

As an initial test of our theory we compute the osmotic pressure of charged protein solutions

$$\Pi = \eta \frac{\partial f}{\partial \eta}. \quad (19)$$

Fig. 2 compares the theory to experimental measurements of bovine serum albumin [21]. We limit our comparison to pH values where the protein charge has been measured [22], however the resulting charge values $q = -20.2$ (pH = 7.3), $q = -9.1$ (pH = 5.4), and $q = 3.2$ (pH = 4.6) cover a sufficiently large range to provide a rigorous test of the model. We use a protein radius of 2.4 nm [23] and the single fitting parameter is $\epsilon = 1.22k_B T = 2.98$ kJ/mol. The agreement is generally good, with an average error of 6.5% for $q = 3.2$ and -9.1 and a

larger 14% error (12% excluding the outlier at 100 g/l) at $q = -20.2$.

In earlier work these data were modeled by fitting an effective protein volume for each pH [24]. These effective volumes ranged from slightly *negative* near the isoelectric point to four-fold greater than the actual volume when the protein carries a charge of ~ 60.0 [25]. Our modeling suggests that these trends can be explained by nonspecific protein binding competing with electrostatic monopole repulsion (mediated by the salt ions).

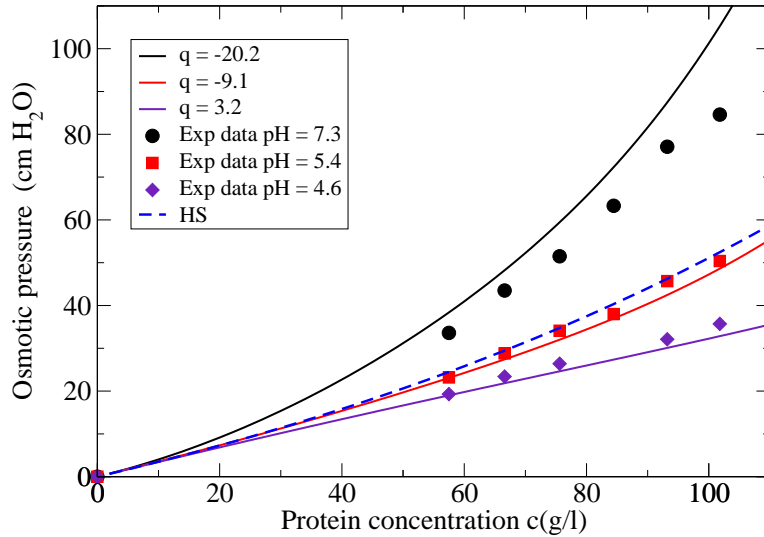


FIG. 2: Plot of osmotic pressure vs. protein concentration for three different protein charges, $q = -20.2$, $q = -9.1$ and $q = 3.2$ (solid lines). Points are data from [21] for three different pH values pH = 7.3, 5.4 and 4.6. The measured protein charges at these pH values are obtained from [22]. $\epsilon = 2.98$ kJ/mol is our fitting parameter. Temperature and salt concentration is same as in the experiment [21].

Fig. 3 shows predictions for the osmotic pressure as a function of salt for two values of the protein charge. Not surprisingly, greater salt concentrations result in lower osmotic pressures. This is explained by the fact that at higher salt concentrations the neutralizing counterions lie closer to the surface of the protein. Therefore, neighboring proteins will impose fewer constraints on the entropy of the screening layers.

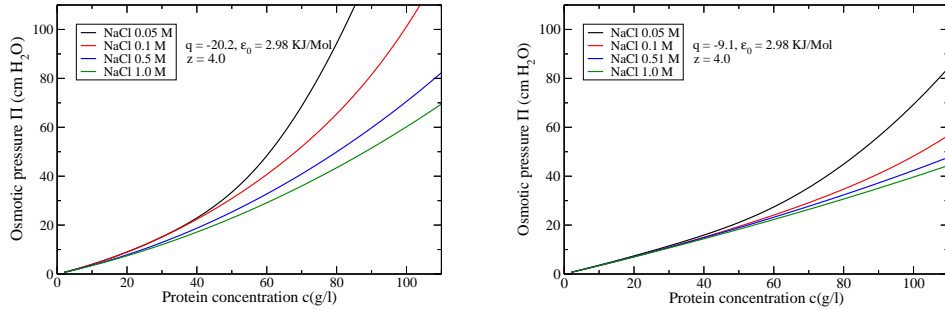


FIG. 3: Plot of osmotic pressure vs. protein concentration for salt concentrations from 0.05M to 1.0M. The two panels are for protein charges $q = -20.2$ (left) and $q = -9.1$ (right).

Fig. 4 shows the component terms of the free energy as a function of the concentration. It is immediately apparent that the coulomb energy is minuscule in comparison with the other terms. This observation is somewhat misleading because the total free energy is a small residual from the addition of large terms with opposing signs. Therefore, the coulomb energy perturbation does give a significant quantitative improvement. On the other hand, if quantitative results are not required, a good estimate of pH and salt effects can be obtained from Eq. 17 while neglecting the more difficult to calculate coulomb energy.

Another observation from Fig. 4 is that the repulsive terms are entropic in origin while the attractive terms are energetic. This has important consequences from the temperature dependence of the pressure. In Fig. 5 we plot the temperature dependence of the osmotic pressure for two systems of hard spheres. The first system interacts by the entropy dominated electrostatic interaction (Eqs. 11 and 17) while the second interacts by a repulsive Yukawa (Debye-Huckel) potential that is energy dominated (calculated using the MSA). We see that the temperature has qualitatively different effects on the two systems. In the Yukawa system the osmotic pressure actually decreases with temperature because the reduced Boltzmann weight given to the repulsive interaction at higher temperatures effectively frees volume for the spheres to explore. It is only with the entropy dominated electrostatic interaction that we recover the physically reasonable result that the osmotic pressure should increase with temperature [26].

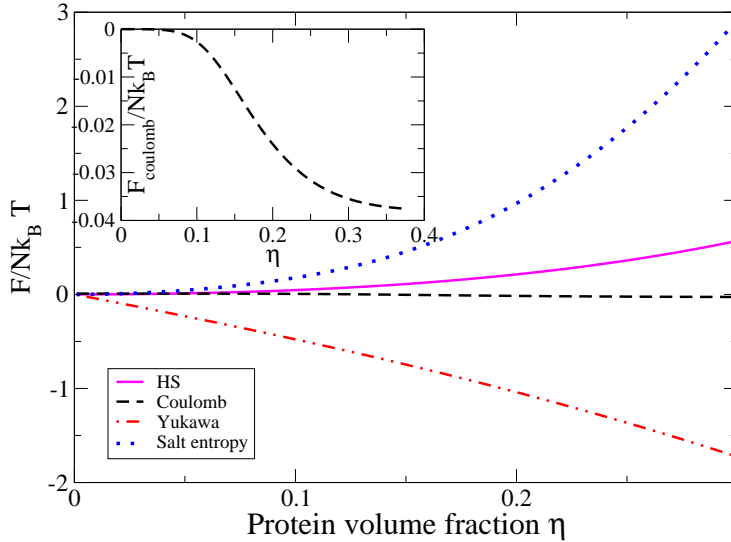


FIG. 4: Plot of the contributions to the free energy $F/NK_B T$. The four curves are f_{hc} (solid), $f_{coulomb}$ (dashes), f_{att} (dot-dash), f_{salt} (dots). The coulomb term is very small (inset) compared to other three terms.

B. Liquid-liquid phase separation

The solution free energy Eq. 1 contains a binding energy term that favors dense states competing with entropic terms that favor dilute states. This means that under some conditions the solution may phase separate in order to maximize the free energy contribution from these extreme states. The conditions for an equilibrium between two phases of unequal densities are

$$\mu'_p = \mu''_p \quad (20)$$

$$\mu'_+ = \mu''_+ \quad (21)$$

$$\mu'_- = \mu''_- \quad (22)$$

where μ' and μ'' are the chemical potential of the dilute and dense phases, respectively, and the subscripts represent proteins, cations, and anions. The conditions for the salt ions are satisfied by Eq. 8 which captures both mixing entropy and coulomb energy contributions

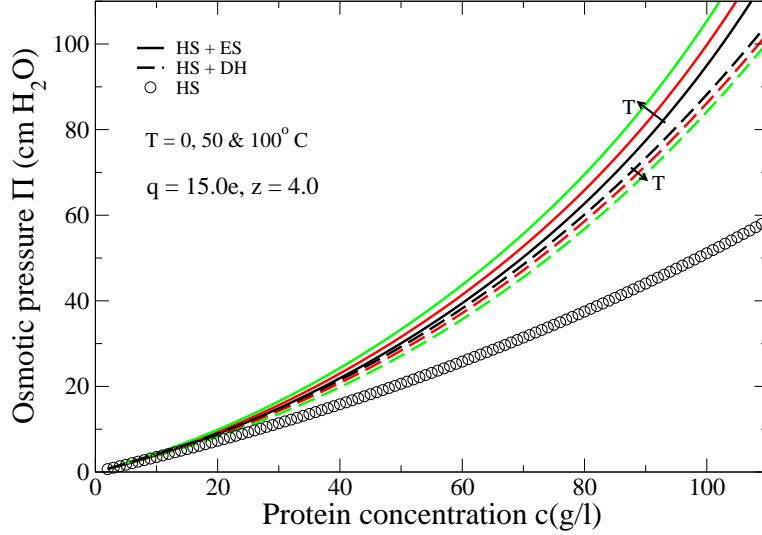


FIG. 5: Plot of osmotic pressure (OP) Π vs. protein concentration η for two different representations of the electrostatic interaction. Solid curves show the OP calculated for hard spheres with the entropy dominated interaction given by Eqs. 11 and 17. The three curves show the expected increase in OP with temperature. The dashed curves show the OP calculated for hard spheres with a Debye-Huckel type electrostatic interaction. This model shows a non-physical decrease in the OP with temperature.

to the chemical potential. Eqs. 21 and 22 are, therefore, built into our free energy. Thus, the slope $\partial F/\partial\eta$ is an effective chemical potential for the protein that includes the effects of maintaining the salt equilibrium.

The densities of coexisting phases are found by numerically searching for a line with two points tangent to $F(\eta)$ [27]. In Fig. 6 we plot the coexistence curve predicted by Eq. 1 for three different NaCl concentrations (3%, 5% and 7% w/v) for a particle of diameter $\sigma = 3.2\text{nm}$ and charge $q = 10.3e$. These parameters correspond to the pH 4.5 conditions used by Muschol and Rosenberger [28] to determine the liquid-liquid binodal curves for lysozyme. The single free parameter, $\epsilon = 3.98 \text{ kJ/mol}$, has been set to reproduce the critical temperature under 7% salt.

It is immediately obvious that the theory fails to capture the width of the lysozyme coexistence curves. This is because proteins have much broader binodal curves than systems of smooth spheres [11]. The reasons for this are not clear, but possible factors include anisotropic or directional binding [29–31], temperature dependence of the short range attraction [13], asphericity [32], and the range of the attraction [14]. However, the theory does a reasonable job of reproducing the salt-dependent shift in the critical temperature, although as we observed with the osmotic pressure, the theory somewhat over-predicts the trend under the most extreme conditions (low salt or high charge).

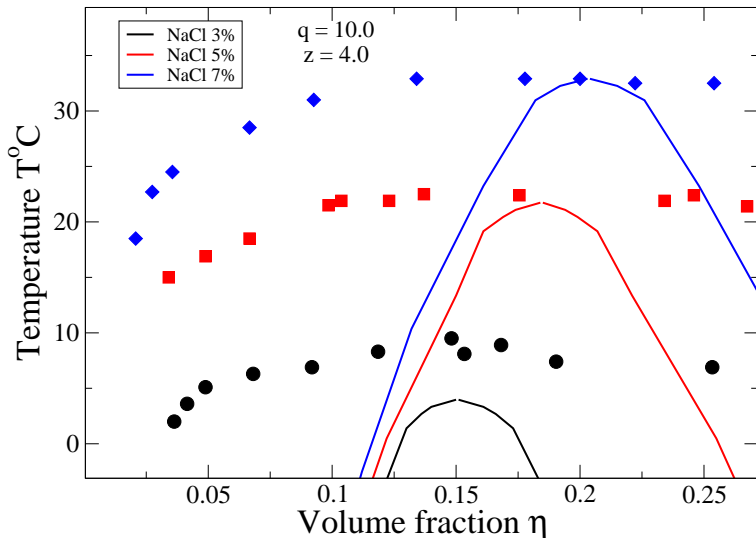


FIG. 6: Plot of liquid-liquid coexistence curve for three different salt concentrations NaCl 3%, 5% and 7%. Data points are experimental curve from [33]. We have good predictions for critical temperature. Other parameters protein charge $q = 10.0$, range of Yukawa interaction $z = 4.0$ and binding energy $\epsilon = 3.98$ kJ/mol. We kept binding energy as our fitting parameter and fixed all other parameters.

A key feature of this theory is the partitioning of ions between the dilute and dense phases by the Donnan effect. However, experiments to observe this partitioning have yielded negative results [28]. Using Eq. 13 we can see why the partitioning was experimentally

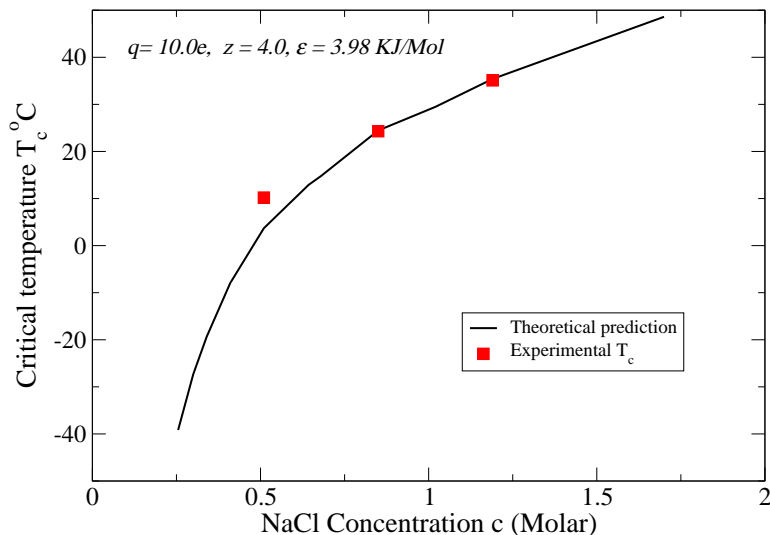


FIG. 7: Plot of critical temperature T_c vs. salt concentration in Molar for protein charge $q = 10.0$

elusive. At pH 4.5 lysozyme has a calculated charge of approximately $Z = +10$. If we take the protein volume to be 17 nm^3 and assume that the dense phase has a density $\eta = 1/3$, then for 0.5M salt conditions Eq. 15 gives a potential of $e\phi/k_B T = 0.46$. From Eq. 8 we get a counterion concentration of $1.58 c_0$ within the solvent fraction of the dense phase. To get the apparent concentration within the total phase we multiply by $1 - \eta$ to account for the excluded volume of the protein. We find that the apparent counterion concentration in the dense phase is nearly unchanged from the bulk value. However, this cancelation is entirely a coincidence of the conditions used in Ref [28]. A similar calculation for the coions yields an apparent concentration of $0.4c_0$, however, this may have been missed due to difficulties associated with the sodium assay [M. Muschol personal communication].

IV. CONCLUSION

We have presented an approximate method for calculating electrostatic effects in dense protein solutions. Our method captures the non-pairwise nature of electrostatic interactions at high concentrations, yet requires only a single particle calculation within a cell model.

Such methods may enable the rational manipulation of protein solution behavior and phase diagrams using pH and salt concentration as control parameters.

Acknowledgments We would like to thank M. Muschol and A. Minton for valuable discussions. This work was supported by KSU startup funds.

Appendix A: Mean Spherical Approximation MSA

The attractive term f_{att} in Eq. 1 can be given by the MSA [15] for a Yukawa fluid. As a second-order type theory, the MSA yield

$$\begin{aligned}
f_{att} &= -\frac{1}{2} \sum_{n=1}^{\infty} \frac{v_n}{n} (\beta\epsilon)^n \\
&= \frac{\alpha_0}{\Phi_0} \beta\epsilon - \frac{z^3}{6\eta} \sum_{n=2}^{\infty} \left(\frac{2^{n-2} - n + 2}{n} \right) X^n \\
&\quad + \frac{z^3}{6\eta} \sum_{n=2}^{\infty} \left(\frac{2^{n-2} - n + 2}{n} \right) \left(1 + \frac{Y}{z\psi} \frac{d}{dY} \right) Y^n
\end{aligned} \tag{A1}$$

where

$$\alpha_0 = \frac{L(z)}{z^2(1-\eta)^2}; \tag{A2}$$

$$L(z) = 12\eta[(1 + \eta/2)z + 1 + 2\eta] \tag{A3}$$

$$S(z) = (1 - \eta)^2 z^3 + 6\eta(1 - \eta)z^3 + 18\eta^2 z - 12\eta(1 + 2\eta) \tag{A4}$$

$$\Phi_0 = \frac{\exp(-z)L(z) + S(z)}{z^3(1-\eta)^3}; \tag{A5}$$

$$\psi = z^2(1-\eta)^2 \frac{1 - \exp(-z)}{\exp(-z)L(z) + S(z)} - 12\eta(1-\eta) \frac{1 - z/2 - (1 + z/2)\exp(-z)}{\exp(-z)L(z) + S(z)} \tag{A6}$$

$$w = \frac{6\eta}{\Phi_0^2} \tag{A7}$$

$$v_n = \frac{2(2^{n-2} - n + 2)w^{n-1}[(1 + z\psi)^n - nz^{n-1}\psi^{n-1} - z^n\psi^n]}{z^{2n-3}\Phi_0^2} \tag{A8}$$

$$X = \frac{(1 + z\psi)w}{z^2} \beta\epsilon \tag{A9}$$

and

$$Y = \left(\frac{w\psi}{z} \right) \beta\epsilon \tag{A10}$$

By doing some algebraic manipulation the free energy takes the simple form

$$f_{att} = \frac{\alpha_0}{\Phi_0} \beta \epsilon - \frac{z^3}{6\eta} \left[\mathcal{F}(X) - \mathcal{F}(Y) - (X - Y) \frac{d\mathcal{F}(Y)}{dY} \right] \quad (\text{A11})$$

where the function $\mathcal{F}(X)$

$$\mathcal{F}(X) = -\frac{1}{4} \ln(1 - 2X) - 2 \ln(1 - X) - \frac{3}{2} X - \frac{1}{(1 - X)} + 1 \quad (\text{A12})$$

and its first derivative is

$$\frac{d\mathcal{F}(X)}{dX} = \frac{X(1 - 3X + 3X^2)}{(1 - 2X)(1 - X)^2}. \quad (\text{A13})$$

Appendix B: Linearized Potential

Here we solve for the ion distributions using the cell approximation. We model the protein as a charged sphere embedded in a spherical cavity of solvent with radius $b = a\eta^{-1/3}$. To do this we need to solve the Poisson-Boltzmann equation

$$\epsilon \nabla_r^2 \Psi(\vec{r}) = -\rho_f(\vec{r}) - e N_A (c_0 e^{-e\Psi(\vec{r})/k_B T} - c_0 e^{e\Psi(\vec{r})/k_B T}). \quad (\text{B1})$$

for the electrostatic potential Ψ . Here ρ_f is the fixed charge distribution on the protein, c_0 is the bulk salt concentration, N_A is Avogadro's constant, and $\epsilon \simeq 80\epsilon_0$ is permeability of water. First, we put the PB equation in dimensionless form

$$\nabla_y^2 \Phi = \sinh(\Phi) \quad (\text{B2})$$

where $\Phi = e_p \Psi / k_B T$ is the dimensionless potential, $y = \kappa r$ is a dimensionless length, and

$$\kappa^2 = \frac{2e_p^2 N_A c_0}{\epsilon_0 \epsilon_w k_B T}. \quad (\text{B3})$$

Now we linearize the potential around the local potential $\Phi(y) = \phi(y) + \phi_0$, so we have

$$\nabla_y^2 \Phi = \sinh(\phi + \phi_0) \quad (\text{B4})$$

$$\simeq \phi \cosh \phi_0 + \sinh \phi_0 \quad (\text{B5})$$

$$\nabla_x^2 \phi = \phi + \tanh \phi_0, \quad (\text{B6})$$

where the new length variable is

$$x = \sqrt{\cosh \phi_0} y \quad (\text{B7})$$

$$= \sqrt{\cosh \phi_0} \kappa r. \quad (\text{B8})$$

The solution to Eq. B6 is

$$\phi(x) = A \frac{e^{-x}}{x} + B \frac{e^x}{x} - \tanh \phi_0, \quad (\text{B9})$$

where the constants A and B are determined by the boundary conditions. The boundary conditions are that at the inner sphere $r = a$ the electric field is equal to that of the bare macroion, and at the outer sphere $r = b$ the electric field vanishes (due to charge neutrality).

After scaling the sphere radii

$$\alpha = \sqrt{\cosh \phi_0} \kappa a \quad (\text{B10})$$

$$\beta = \sqrt{\cosh \phi_0} \kappa b \quad (\text{B11})$$

the inner boundary condition becomes

$$-E_0 = \frac{d\phi}{dx} \quad (\text{B12})$$

$$= -A \frac{e^{-\alpha}}{\alpha} \left(1 + \frac{1}{\alpha}\right) + B \frac{e^{\alpha}}{\alpha} \left(1 - \frac{1}{\alpha}\right), \quad (\text{B13})$$

where the dimensionless electric field is

$$E_0 = \frac{q e_p \kappa \sqrt{\cosh \phi_0}}{4\pi \epsilon k_B T \alpha^2}, \quad (\text{B14})$$

where $q e_p$ is the charge on the central sphere. At the outer sphere boundary we have

$$-A \frac{e^{-\beta}}{\beta} \left(1 + \frac{1}{\beta}\right) + B \frac{e^{\beta}}{\beta} \left(1 - \frac{1}{\beta}\right) = 0, \quad (\text{B15})$$

from which we derive

$$B = A e^{-2\beta} \frac{1 + 1/\beta}{1 - 1/\beta}. \quad (\text{B16})$$

Combining Eqs. B13 and B16 we find

$$A[-e^{-\alpha}(\alpha + 1)(\beta - 1) + e^{\alpha-2\beta}(\alpha - 1)(\beta + 1)] = -\alpha^2 E_0(\beta - 1). \quad (\text{B17})$$

So the two constants are

$$A = \frac{\alpha^2 E_0 e^{\beta}(\beta - 1)}{e^{-\alpha+\beta}(\alpha + 1)(\beta - 1) - e^{\alpha-\beta}(\alpha - 1)(\beta + 1)} \quad (\text{B18})$$

$$B = \frac{\alpha^2 E_0 e^{-\beta}(\beta + 1)}{e^{-\alpha+\beta}(\alpha + 1)(\beta - 1) - e^{\alpha-\beta}(\alpha - 1)(\beta + 1)}. \quad (\text{B19})$$

The total potential is then

$$\Phi(x) = \phi(x) + \phi_0 \quad (\text{B20})$$

$$= \frac{\alpha^2 E_0}{e^{-\alpha+\beta}(\alpha+1)(\beta-1) - e^{\alpha-\beta}(\alpha-1)(\beta+1)} \left(\frac{e^{\beta-x}(\beta-1)}{x} + \frac{e^{x-\beta}(\beta+1)}{x} \right) - \tanh \phi_0 + \phi_0, \quad (\text{B21})$$

so the constant used in the text is

$$C = \frac{\alpha^2 E_0}{e^{-\alpha+\beta}(\alpha+1)(\beta-1) - e^{\alpha-\beta}(\alpha-1)(\beta+1)}. \quad (\text{B22})$$

The coulomb energy is obtained as follows

$$f_{\text{coulomb}} = \frac{\epsilon}{2} \int_{\alpha}^{\beta} |\vec{E}(\vec{r})|^2 d^3 r \quad (\text{B23})$$

$$= \int_{\alpha}^{\beta} \left[\frac{1}{x^2} (A_1^2 e^{-2x} + 2A_1 B_1 + B_1^2 e^{2x}) - \frac{2}{x} (-A_1^2 e^{-2x} + B_1^2 e^{2x}) + (A_1^2 e^{-2x} + B_1^2 e^{2x} - 2A_1 B_1) \right] dx \quad (\text{B24})$$

$$= \left[-\frac{1}{x} (A_1 e^{-x} + B_1 e^x)^2 + \frac{1}{2} (B_1^2 e^{2x} - A_1^2 e^{-2x} - 4A_1 B_1 x) \right]_{\alpha}^{\beta} \quad (\text{B25})$$

$$= -2C^2 \beta^3 + \frac{C^2}{\alpha} ((\beta-1)e^{-\alpha+\beta} + (\beta+1)e^{\alpha-\beta})^2 - \frac{C^2}{2} ((\beta+1)^2 e^{2(\alpha-\beta)} - (\beta-1)^2 e^{-2(\alpha-\beta)} - 4(\beta^2 - 1)\alpha) \quad (\text{B26})$$

where $A_1 = C(\beta-1) \exp(\beta)$ and $B_1 = C(\beta+1) \exp(-\beta)$.

-
- [1] Zimmerman, Steven B and Minton, Allen P, Annual review of biophysics and biomolecular structure, 27, **22**, 1993
 - [2] Shire, Steven J and Shahrokh, Zahra and Liu, Jun, Journal of pharmaceutical sciences, 6, 1390, **93**, 2004
 - [3] Mcpherson, Alexander, Methods (San Diego, Calif.), 3, 254, **34**, 2004
 - [4] Tavares, Frederico W. and Bratko, D. and Blanch, Harvey W and Prausnitz, John M., J. Phys. Chem. B, 26, 9228, **108**, 2004
 - [5] Elcock, Adrian H and McCammon, J. Andrew, Biophysical journal, 2, 613, **80**, 2001
 - [6] Coen, Cj and Newman, J and Blanch, Harvey W Hw and Prausnitz, John M., Journal of colloid and interface science, 1, 276, **177**, 1996

- [7] Schmit, Jeremy David and Whitelam, Stephen and Dill, Ken A, The Journal of Chemical Physics, 8, 085103, **135**, 2011
- [8] ten Wolde, P. R. and Frenkel, Daan, Science, 5334, 1975, **277**, 1997
- [9] Hagen, M. H. J. and Frenkel, Daan, The Journal of Chemical Physics, 5, 4093, **101**, 1994
- [10] Lomakin, Aleksey and Asherie, Neer and Benedek, George B., Proceedings of the National Academy of Sciences of the United States of America, 18, 10254, **100**, 2003
- [11] Lomakin, Aleksey and Asherie, Neer and Benedek, George B., The Journal of Chemical Physics, 4, 1646, **104**, 1996
- [12] Asherie, N and Lomakin, A and Benedek, George B., Phys. Rev. Lett., 23, 4832, **77**, 1996
- [13] Gögelein, Christoph and Nägele, Gerhard and Tuinier, Remco and Gibaud, Thomas and Stradner, Anna and Schurtenberger, Peter, The Journal of chemical physics, 8, 085102, **129**, 2008
- [14] Fu, Dong and Li, Yigui and Wu, Jianzhong, Physical Review E, 1, 38, **68**, 2003
- [15] Tang, Yiping, The Journal of Chemical Physics, 9, 4140, **118**, 2003
- [16] Durand-Vidal, S. and Simonin, J.-P. and Turq, P., Springer, Electrolytes at Interfaces (Progress in Theoretical Chemistry and Physics), 2000
- [17] Duh, D.M. and Mier-Y-Teran, L, Molecular Physics, 3, 373, **90**, 1997
- [18] Carnahan, N.F. and Starling, K.E., The Journal of Chemical Physics, 635, **51**, 1969
- [19] Wall, F. T. and Berkowitz, Joan, The Journal of Chemical Physics, 1, 114, **26**, 1957
- [20] Levin, Yan and Trizac, Emmanuel and Bocquet, Lydéric, Journal of Physics: Condensed Matter, 48, S3523, **15**, 2003
- [21] Kanal, K M and Fullerton, G D and Cameron, I L, Biophysical journal, 1, 153, **66**, 1994
- [22] Vilker, V.L. and Colton, C.K. and Smith, K.A., Journal of Colloid and Interface Science, 2, 548, **79**, 1981
- [23] Minton, Allen P. and Edelhoich, H., Biopolymers, 2, 451, **21**, 1982
- [24] Minton, Allen P., Biophysical chemistry, 1, 65, **57**, 1995
- [25] Salis, Andrea and Boström, Mathias and Medda, Luca and Cugia, Francesca and Barse, Brajesh and Parsons, Drew F and Ninham, Barry W and Monduzzi, Maura, Langmuir : the ACS journal of surfaces and colloids, 18, 11597, **27**, 2011
- [26] Piazza, Roberto, J. Cryst. Growth, 2-4, 415, **196**, 1999
- [27] Chaikin, P. M. and Lubensky, T.C., Cambridge University Press, Principles of Condensed

Matter Physics, 2000

- [28] Muschol, Martin and Rosenberger, Franz, J. Chem. Phys., 6, 1953, **107**, 1997
- [29] Kern, Norbert and Frenkel, Daan, J. Chem. Phys., 21, 9882, **118**, 2003
- [30] Bianchi, Emanuela and Tartaglia, Piero and Zaccarelli, Emanuela and Sciortino, Francesco, J Chem Phys, 14, 144504, **128**, 2008
- [31] Liu, Hongjun and Kumar, Sanat K and Sciortino, Francesco and Evans, Glenn T, J. Chem. Phys., 4, 044902, **130**, 2009
- [32] , Wang, Ying and Lomakin, Aleksey and Latypov, Ramil F and Benedek, George B., Proceedings of the National Academy of Sciences of the United States of America, 40, 16606, **108**, 2011
- [33] Muschol, Martin and Rosenberger, Franz, J. Chem. Phys., 24, 10424, **103**, 1995